Ⅲ. AT 患者全国調査から明らかになった臨床症状

1. 発症年齢，診断年齢（疾患名にとらわれると診断が遅れる）

小脳失調が明らかになった年齢の中央値（範囲）は18カ月（8カ月～5歳6カ月）であり，毛細血管拡張は6歳8カ月（1歳8カ月～13歳6カ月）に観察されている。診断は6歳9カ月（11カ月～24歳6カ月）時になされているが，おそらくは毛細血管拡張とあわせて臨床診断となっているものと思われる。これらの年齢は Cabana MD らの報告[5]と大きな差はない。

注意すべきは毛細血管拡張は半数が6歳以上となってから明らかになることであり，Ataxia telangiectasia という疾患名にとらわれると診断時期が遅くなり，X線撮影や悪性腫瘍に対する化学療法などに際して払うべき注意が行えなくなる可能性がある。2歳以降の小脳失調症で α fetoprotein が高値であれば，AT を積極的に疑う必要がある（表2の診断の手引きを参照）。

生存者の年齢の中央値（範囲）は14歳5カ月（4歳～28歳7カ月），逝去者では19歳0カ月（5歳9カ月～31歳10カ月）であった。また生存年齢中央値は26.0歳である。

2. 神経症状（図1）

まとめを図1に示す。全員で体幹失調を認め，注意深い観察あるいは補助器具を用いれば眼球失行（apraxia）も明らかである。舞踏病も3割程度で認められ注意を要する。

表2　AT の診断基準（AT Children's Project HP）
（http://www.communityatcp.org/NETCOMMUNITY/Page.aspx?pid=590&srcid=588より改変）

［症状］

1．歩行開始と共に明らかになる歩行失調（体幹失調）：必発症状
　徐々に確実に進行（2歳から5歳までの間には進行がマスクされることもある）．
2．小脳性構語障害・流涎
3．眼球運動の失行，眼振
4．舞踏病アテトーゼ（全例ではない）
5．低緊張性顔貌
6．眼球結膜・皮膚の毛細血管拡張
　←6歳までに50%，8歳時で90%が明らかに．
7．免疫不全症状（反復性気道感染症）
　←30%では免疫不全症状を認めない．
8．悪性腫瘍：発生頻度が高い．
9．そのほか（認めることがあるもの）：
　発育不良
　内分泌異常（耐糖能異常：インスリン非依存性糖尿病），
　皮膚，頭髪，血管の早老性変化

［検査データ］

1．α フェトプロテインの上昇（2歳以降：95%以上で）
2．CEA の増加（認めることがある）
3．IgG（IgG 2），IgA，（IgE）の低下（70%で）
4．CD 4 細胞中CD4+CD45RA+細胞の比率の低下
5．そのほか：
　電離放射線高感受性
　リンパ球，線維芽細胞の染色体異常

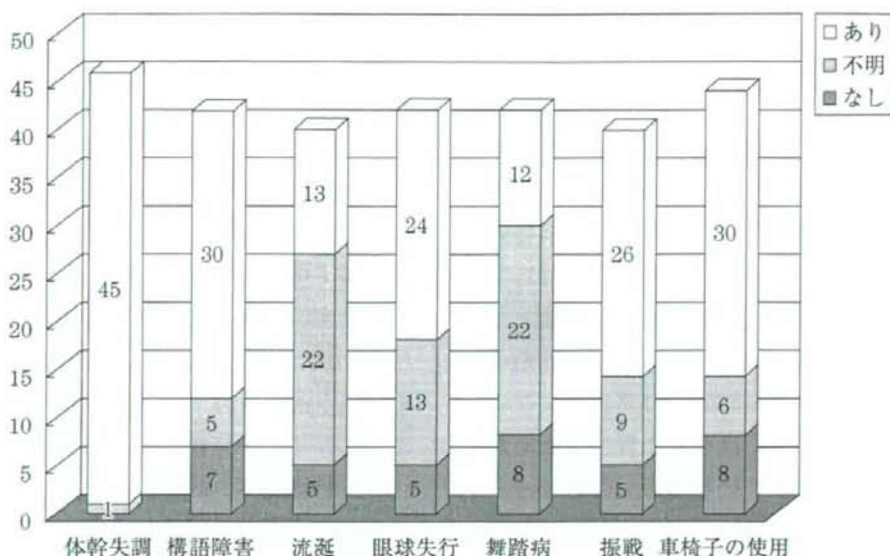

図1　神経症状

誤嚥性肺炎などから嚥下障害の評価は重要であり，Johns Hopkins 大学の AT センターでは嚥下無呼吸（deglutition apnea）の持続と嚥下前後の呼気流量を測定することにより管理に役立てているようである。

3．悪性腫瘍

悪性腫瘍は76名中17例に発症し，12症例で詳細な情報が得られた。6例は急性リンパ性白血病（T：4例，PreB：2例），4例は悪性リンパ腫，1例が組織球症，1例は胆管癌である。このうち発症後1年の時点で寛解に入っていたのは T-ALL の2症例と，悪性リンパ腫の1例のみである。予想されることではあるが，化学療法薬に対する有害事象も目立ち，急激な多臓器不全，心不全，遅発性出血性膀胱炎などを認めている点に注意を要する。特に，PreB-ALL の発症は AT の診断前であることも経験する。

4．感染症

AT では日和見感染症が稀とされている[6]。実際に感染症は神経症状が進んでからの誤嚥性肺炎など細菌感染症が前面に立っている。AT ではT細胞減少症を認めることが多く，検査データからは予想に反する結果といえる。今回の解析からは，AT では持続性 EBV 感染症，難治性 VZV 感染症，ヘルペス脳炎などヘルペス属感染症が重症化することが明らかになった。また長期入院を要する麻疹肺炎も2症例で認められている。CMV 感染症，カリニ肺炎，真菌感染症は稀だが，早期からの細菌感染症などにマスクされているだけの可能性もあり注意が必要と考えられる。

5．免疫異常

AT では CD3＋，CD4＋，CD8＋，CD20＋細胞の減少はそれぞれ66%，76%，39%，78%で認められた。CD4＋CD45RA＋細胞の減少も特徴的である。T細胞減少を反映して TREC（T cell receptor excision circle）は全例で低下していた（既報と一致する[7]）。T細胞減少はまた，上記の重症ウイルス感染症と相関が認められた。

免疫グロブリンでは16%で IgG<500mg/dℓ，34%で IgA<50mg/dℓであった。低 IgG 血症のうち，3例は panhypogammaglobulinemia であり，5例は HyperIgM の表現型をとっていた。これらの患者では CD27陽性メモリーB細胞数が低下していた。免疫異常は進行性ではないことが示されている[6]。

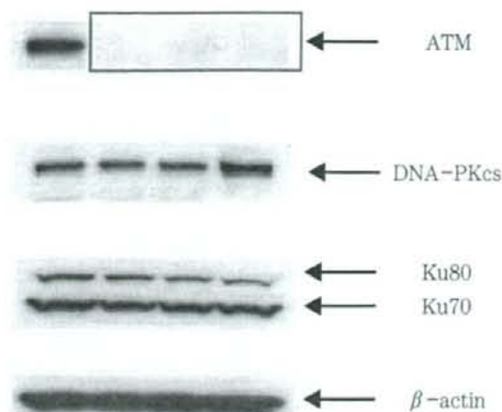

図2　AT の診断（anti-ATM immunoblot）
第一レーンは正常コントロール，第二から四レーンはAT患者サンプル．

6．診断（図2）

ATM は66の exon からなる長大な遺伝子であり，また患者での変異は intron 領域にも多いため，その塩基配列決定には大きな労力を要していたが，現在は PIJD を通じて ATM の遺伝子解析が可能である。しかし診断のうえで欠かせないのが，Westernblot 法による ATM タンパクの確認であり，当施設ではT細胞を *in vitro* で増殖させるか，あるいは EBV-LCL を作成して実施している。この際には ATR，Mre11，Rad50，NBS 1，Ku70/80，DNA-PKcs も解析し，漏れのないようにしている。

最近教室の高木らは，電離放射線照射あるいは H_2O_2 刺激後の ATM リン酸化を FA-CS で測定する系を立ち上げた（Leukemia，in press）。この方法は簡便で半日以内に結果が出るのみならず，hetero 異常も検出可能である。スクリーニングとしては最適の方法と考えている。

7．死亡原因

死因の第一位は感染症である。今回のアンケートでは感染症で死亡した18名のうち5例が化学療法中になくなっている。そのほか，腫瘍死も3名と目立っている。何よりも誤嚥性肺炎対策が急務と考える。

おわりに

AT の臨床症状を中心に概説した。AT は神経医により気づかれるが，初期診断には難渋することがある。その点で，αFP を参考にしつつ，phospho-ATM FACS などで第一次スクリーニングとすることが大切であろう。AT と判明したら，血液腫瘍医，内分泌専門医などとの連携が必須である。ATM についての基礎研究の進歩は目覚ましいが，小脳失調の発症原因解明など神経分野での検討が立ち遅れている。今後この領域に神経医が参画することを期待したい。

特に治療の開発が遅れている。酸化防止薬としての N-acetyl cysteine や，exon skipping をブロックする antisence morpholino による治療，readthrough を狙った治療などが試みられているが，実用には不十分である。

私どもの施設は日本の AT 診断センターに指定されていて，診断や治療について相談に応じている。神経症状の評価については，都立神経病院神経小児科 熊田聡子医師が国際ワークショップでトレーニングを受けてきている。何かの際にはご連絡いただければ幸いである。また実際のフォローに際しては，AT Children's Project HP（http://www.atcp.org/）に詳しい情報が掲載されており，ぜひ参照していただきたい。

文　献

1) Gatti RA, Becker-Catania S, Chun HH et al：The pathogenesis of ataxia-telangiectasia. Learning from a Rosetta Stone. Clin Rev Allergy Immunol　20：87～108, 2001
2) Perlman S, Becker-Catania S, Gatti RA：Ataxia-telangiectasia：diagnosis and treatment. Semin Pediatr Neurol　10：173～182, 2003
3) Shiloh Y：The ATM-mediated DNA-damage response：taking shape. Trends Biochem Sci

31：402～410, 2006
4) Pan-Hammarstrom Q, Dai S, Zhao Y et al：ATM is not required in somatic hypermutation of VH, but is involved in the introduction of mutations in the switch mu region. J Immunol 170：3707～3716, 2003
5) Cabana MD, Crawford TO, Winkelstein JA, Christensen JR, Lederman HM：Consequences of the delayed diagnosis of ataxia-telangiectasia. Pediatrics 102：98～100, 1998
6) Claret Teruel G, Giner Munoz MT, Plaza Martin AM, Martin Mateos MA, Piquer Gibert M, Sierra Martinez JI：Variability of immunodeficiency associated with ataxia telangiectasia and clinical evolution in 12 affected patients. Pediatr Allergy Immunol 16：615～618, 2005
7) Giovannetti A, Mazzetta F, Caprini E et al：Skewed T-cell receptor repertoire, decreased thymic output, and predominance of terminally differentiated T cells in ataxia telangiectasia. Blood 100：4082～4089, 2002

Cell

Tyrosine Kinases Btk and Tec Regulate Osteoclast Differentiation by Linking RANK and ITAM Signals

Masahiro Shinohara,[1,2] Takako Koga,[1,2] Kazuo Okamoto,[1,2] Shinya Sakaguchi,[4] Kimiko Arai,[1,5] Hisataka Yasuda,[7] Toshiyuki Takai,[6] Tatsuhiko Kodama,[8] Tomohiro Morio,[3] Raif S. Geha,[9] Daisuke Kitamura,[10] Tomohiro Kurosaki,[11] Wilfried Ellmeier,[4] and Hiroshi Takayanagi[1,2,*]

[1]Department of Cell Signaling, Graduate School
[2]Center of Excellence Program for Frontier Research on Molecular Destruction and Reconstruction of Tooth and Bone
[3]Department of Pediatrics and Developmental Biology, Graduate School
Tokyo Medical and Dental University, Yushima 1-5-45, Bunkyo-ku, Tokyo 113-8549, Japan
[4]Institute of Immunology, Center for Physiology, Pathophysiology, and Immunology, Medical University of Vienna, Lazarettgasse 19, Vienna 1090, Austria
[5]Division of Orthodontics and Dentofacial Orthopedics, Graduate School of Dentistry
[6]Department of Experimental Immunology, Institute of Development, Aging, and Cancer
Tohoku University, Seiryo-machi 4-1, Aoba-ku, Sendai, Miyagi 980-8575, Japan
[7]Nagahama Institute for Biochemical Science, Oriental Yeast Co., Ltd., Kanoh-cho 50, Nagahama, Shiga 526-0804, Japan
[8]Department of Molecular Biology and Medicine, Research Center for Advanced Science and Technology, University of Tokyo, Komaba 4-6-1, Meguro-ku, Tokyo 153-8904, Japan
[9]Division of Immunology, Children's Hospital, One Blackfin Circle, Boston, MA 02115, USA
[10]Division of Molecular Biology, Research Institute for Biological Sciences, Tokyo University of Science, Yamazaki 2669, Noda, Chiba 278-0022, Japan
[11]Laboratory for Lymphocyte Differentiation, RIKEN Research Center for Allergy and Immunology, RIKEN Yokohama Institute, Suehiro-cho 1-7-22, Tsurumi-ku, Yokohama, Kanagawa 230-0045, Japan
*Correspondence: taka.csi@tmd.ac.jp
DOI 10.1016/j.cell.2007.12.037

SUMMARY

Certain autoimmune diseases result in abnormal bone homeostasis, but association of immunodeficiency with bone is poorly understood. Osteoclasts, which derive from bone marrow cells, are under the control of the immune system. Differentiation of osteoclasts is mainly regulated by signaling pathways activated by RANK and immune receptors linked to ITAM-harboring adaptors. However, it is unclear how the two signals merge to cooperate in osteoclast differentiation. Here we report that mice lacking the tyrosine kinases Btk and Tec show severe osteopetrosis caused by a defect in bone resorption. RANK and ITAM signaling results in formation of a Btk(Tec)/BLNK(SLP-76)-containing complex and PLCγ-mediated activation of an essential calcium signal. Furthermore, Tec kinase inhibition reduces osteoclastic bone resorption in models of osteoporosis and inflammation-induced bone destruction. Thus, this study reveals the importance of the osteoclastogenic signaling complex composed of tyrosine kinases, which may provide the molecular basis for a new therapeutic strategy.

INTRODUCTION

Bone homeostasis depends on balanced action of bone-resorbing osteoclasts and bone-forming osteoblasts (Karsenty and Wagner, 2002). Tipping the balance in favor of osteoclasts leads to diseases with a low bone mass, whereas impaired osteoclastic bone resorption results in diseases with a high bone mass, including osteopetrosis (Teitelbaum and Ross, 2003). Bone reserves calcium and responds to calcium-regulating hormones, but osteoclasts and osteoblasts are not only regulated by the endocrine system. The immune and bone systems share numerous regulatory factors, including cytokines, receptors, signaling molecules, and transcription factors (Theill et al., 2002; Walsh et al., 2006; Takayanagi, 2007). Therefore, the pathology of one system may very well affect the other: it is well documented that enhanced bone resorption is associated with activation of the immune system observed in autoimmune or inflammatory diseases such as rheumatoid arthritis and periodontitis (Theill et al., 2002; Takayanagi, 2007).

Diseases with impaired immune responses are also associated with bone abnormalities, but it is poorly understood how the immunodeficiencies are functionally related to bone disorders. Hyperimmunoglobulin E (IgE) syndrome is characterized by skeletal symptoms such as osteoporosis (Kirchner et al., 1985) and scoliosis (Grimbacher et al., 1999), which are partly explained by the abnormality of osteoblasts and osteoclasts

caused by the mutation in the *STAT3* gene. (Minegishi et al., 2007). X-linked hyper-IgM syndrome (caused by a mutation in the *CD40L* gene) has a skeletal complication, osteopenia, which is attributed to enhanced osteoclast formation due to the impaired production of interferon-γ by T cells (Lopez-Granados et al., 2007). Thus, exploring the mechanisms underlying skeletal complications in primary immunodeficiencies will be important for understanding the shared mechanisms and crosstalk between immune and bone systems.

The osteoclast was the first skeletal cell to be determined to be under the control of the immune system (Horton et al., 1972). Because osteoclasts originate from bone marrow-derived monocyte/macrophage precursor cells (BMMs) of hematopoietic lineage, many regulators of osteoclast differentiation are also utilized in the control of the innate and adaptive immune systems. The differentiation of osteoclasts is mainly regulated by three signaling pathways activated by receptor activator of nuclear factor-κB ligand (RANKL), macrophage colony-stimulating factor (M-CSF), and immunoreceptor tyrosine-based activation motif (ITAM) (Asagiri and Takayanagi, 2007). Whereas M-CSF promotes the proliferation and survival of BMMs (Ross and Teitelbaum, 2005), RANKL activates the differentiation process by inducing the master transcription factor for osteoclastogenesis, nuclear factor of activated T cells c1 (NFATc1), via the tumor necrosis factor receptor-associated factor 6 (TRAF6) and c-Fos pathways (Takayanagi et al., 2002). The induction of NFATc1 is also dependent on the calcium signal, which is mediated by the activation of ITAM in adaptor molecules such as DNAX-activating protein 12 (DAP12) and Fc receptor common γ subunit (FcRγ) (Koga et al., 2004; Mocsai et al., 2004) in association with costimulatory receptors of the immunoglobulin superfamily, including triggering receptor expressed in myeloid cells-2 (TREM-2), signal-regulatory protein β1 (SIRPβ1), paired immunoglobulin-like receptor-A (PIR-A), and osteoclast-associated receptor (OSCAR) (Koga et al., 2004). Phosphorylation of ITAM results in recruitment of the nonreceptor tyrosine kinase Syk, leading to the activation of phospholipase Cγ (PLCγ) and calcium mobilization (Faccio et al., 2003; Koga et al., 2004; Mocsai et al., 2004; Mao et al., 2006), but osteoclastogenesis cannot be induced by costimulatory signals alone and requires RANKL stimulation. However, it has been unclear how RANK and ITAM signals merge to cooperatively stimulate the downstream signaling pathway.

To identify the molecules activated by RANKL that stimulate the calcium signaling pathway by functioning as an integrator of the RANK and ITAM signals, we focused on nonreceptor tyrosine kinases because PLCγ initiates the calcium signal after tyrosine phosphorylation. Among the nonreceptor tyrosine kinases, genome-wide screening revealed Btk and Tec to be highly expressed in osteoclasts. The Tec kinase family, consisting of Bmx, Btk, Itk, Rlk, and Tec, is preferentially expressed in the hematopoietic system. T cell receptor (TCR) and B cell receptor (BCR) signaling complexes include Itk/Rlk and Tec/Btk, respectively (Schmidt et al., 2004). The role of Btk in antibody production is well recognized by the existence of immunodeficiencies, X-linked agammaglobulinemia (XLA) in humans (Tsukada et al., 1993) and X-linked immunodeficiency (Xid) in mice (Kerner et al., 1995), caused by a mutation in the *Btk* gene; in addition, mice with a combined deficiency of Tec family kinases display both unique and redundant functions in B cells (Btk and Tec) (Ellmeier et al., 2000) and T cells (Itk and Rlk) (Schaeffer et al., 1999). Here we report the crucial role of Btk and Tec in RANKL-induced osteoclastogenesis based on the genetic evidence obtained from $Tec^{-/-}Btk^{-/-}$ mice. In response to RANKL stimulation, Btk and Tec kinases form a signaling complex required for osteoclastogenesis with adaptor molecules such as BLNK, which also recruits Syk, thus linking the RANK and ITAM signals to phosphorylate PLCγ. This study provides a clear example of immunodeficiency association with abnormal bone homeostasis owing to defects in signaling molecules shared by B cells and osteoclasts. Moreover, therapeutic models suggest that suppression of Tec kinases can serve as a molecular basis for the development of future therapeutic strategies against bone diseases.

RESULTS

Osteoclasts Selectively Express Btk and Tec among Tec Kinases

RANK and ITAM signals cooperate to induce calcium signaling, but it has been unknown how these two signals are integrated. To gain insight into the molecules activated by RANKL that are potentially involved in the activation of tyrosine phosphorylation of the PLCγ pathway, we performed a genome-wide screening of mRNAs for nonreceptor tyrosine kinases expressed during osteoclast and osteoblast differentiation (Figure 1A). We identified high expression of *Src* and *Syk*, whose crucial functions in the osteoclast lineage have been well documented (Soriano et al., 1991; Faccio et al., 2003; Koga et al., 2004). Interestingly, osteoclasts, but not osteoblasts, express the mRNAs for *Btk* and *Tec* at a higher level than that for *Src* (Figure 1A). The selective expression of Btk and Tec in osteoclast precursor cells was also confirmed by RT-PCR (Figure 1B) and immunoblot analysis (Figure 1C).

Osteopetrotic Phenotype of Mice Doubly Deficient in Btk and Tec

The results led us to analyze the bone phenotype of mice deficient in Tec (Ellmeier et al., 2000), Btk (Kerner et al., 1995), or both (Ellmeier et al., 2000). Microradiological analysis revealed the trabecular bone volume to be normal in $Tec^{-/-}$ mice, minimally increased in $Btk^{-/-}$ mice, and markedly increased in $Tec^{-/-}Btk^{-/-}$ mice (Figure 1D). Microcomputed tomography clearly indicated that the bone volume was greatly enhanced in $Tec^{-/-}Btk^{-/-}$ mice (Figure 1E). Histological analysis revealed the osteoclast number was significantly reduced in the epiphyseal region, and the bone marrow was abnormally filled with trabecular bone in $Tec^{-/-}Btk^{-/-}$ mice (Figure 1F). We also observed cartilage remnants characteristic of osteopetrosis in $Tec^{-/-}Btk^{-/-}$ mice (Figure 1F). Bone morphometric analysis indicated an increase in bone volume associated with a reduced osteoclast number, a decrease in the indicators of osteoclastic bone resorption (Figure 1G), and a normal level of bone formation in $Tec^{-/-}Btk^{-/-}$ mice (Figure 1H). There was no significant difference in the resorption and formation parameters among the wild-type (WT), $Tec^{-/-}$, and $Btk^{-/-}$ mice (see Figure S1 available online). These results collectively suggest that the increase in bone mass in $Tec^{-/-}Btk^{-/-}$ mice is caused by impaired osteoclastic bone resorption owing to a defect in osteoclast differentiation.

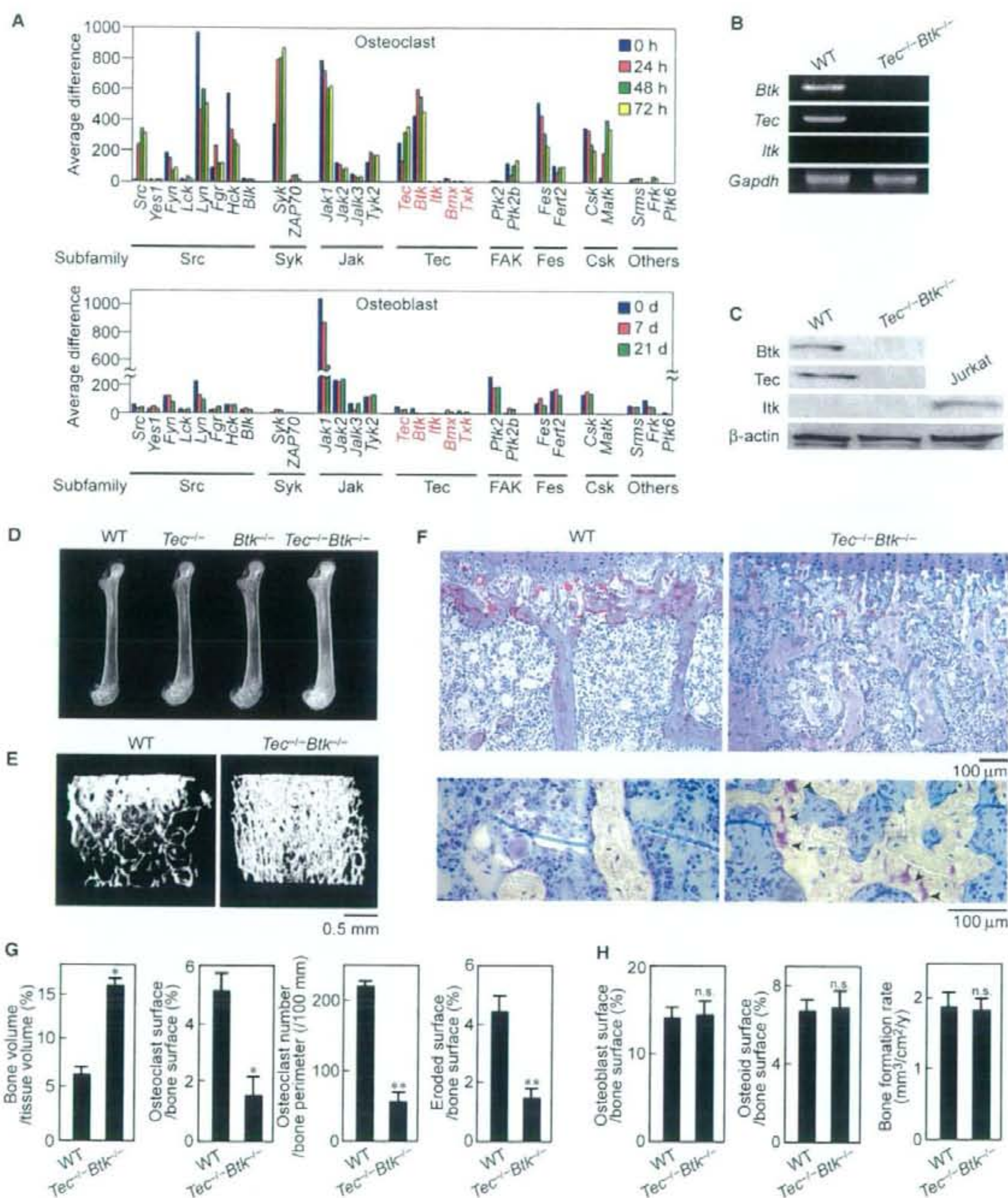

Figure 1. Osteopetrotic Phenotype of $Tec^{-/-}Btk^{-/-}$ Mice

(A) GeneChip analysis of mRNAs for nonreceptor tyrosine kinases during osteoclast and osteoblast differentiation. FAK, focal adhesion kinase; Fes, feline sarcoma oncogene; Csk, c-src tyrosine kinase.

(B) RT-PCR analysis of *Tec*, *Btk*, and *Itk* mRNAs in WT and $Tec^{-/-}Btk^{-/-}$ BMMs.

(C) Expression of Tec, Btk, and Itk proteins in WT and $Tec^{-/-}Btk^{-/-}$ BMMs.

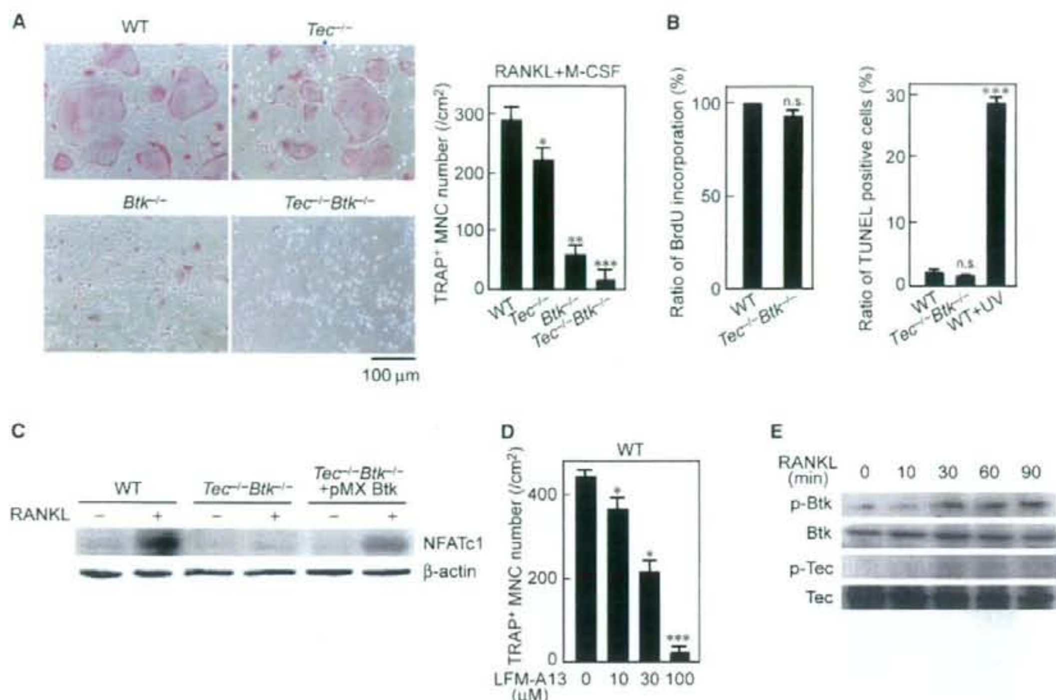

Figure 2. Crucial Role of Tec Family Kinases in RANKL-Induced Osteoclast Differentiation

(A) Osteoclast differentiation from WT, $Tec^{-/-}$, $Btk^{-/-}$, and $Tec^{-/-}Btk^{-/-}$ BMMs in response to RANKL and M-CSF.

(B) Cell proliferation rate (BrdU incorporation assay) and apoptosis (TUNEL assay) of WT and $Tec^{-/-}Btk^{-/-}$ BMMs stimulated with RANKL and M-CSF.

(C) NFATc1 induction in WT and $Tec^{-/-}Btk^{-/-}$ BMMs 72 hr after RANKL stimulation. Retroviral introduction of Btk into $Tec^{-/-}Btk^{-/-}$ BMMs recovers the NFATc1 induction.

(D) Effect of the Tec kinase inhibitor LFM-A13 on the osteoclast differentiation induced by RANKL and M-CSF.

(E) Phosphorylation of Btk and Tec in BMMs in response to RANKL.

Despite the severe defect in osteoclastic bone resorption, the $Tec^{-/-}Btk^{-/-}$ mice had normal tooth eruption, but the results nevertheless suggest that the two kinases play a critically important role in osteoclast differentiation.

Btk and Tec Are Activated by RANKL and Indispensable for Osteoclastogenesis

In vitro osteoclast differentiation was evaluated by counting the multinucleated cells (MNCs) positive for the osteoclast marker tartrate-resistant acid phosphatase (TRAP) after stimulation of BMMs with recombinant RANKL in the presence of M-CSF. Osteoclast differentiation was only minimally affected in $Tec^{-/-}$ cells but was severely impaired in $Btk^{-/-}$ cells and almost completely abrogated in $Tec^{-/-}Btk^{-/-}$ cells (Figure 2A). There was no significant difference in M-CSF-dependent proliferation of precursor cells or the rate of apoptosis between WT and $Tec^{-/-}Btk^{-/-}$ cells (Figure 2B) or in the number of CD11b+ cells in the M-CSF-stimulated bone marrow cells (data not shown). Therefore, there is no defect in the generation of osteoclast precursor cells in $Tec^{-/-}Btk^{-/-}$ mice, although we observed that the survival of mature macrophages derived from $Tec^{-/-}Btk^{-/-}$ mice was partly impaired when cultured with a low concentration of M-CSF (W.E., unpublished data). RANKL-stimulated induction of NFATc1, the key transcription factor for osteoclastogenesis, was severely suppressed in $Tec^{-/-}Btk^{-/-}$ cells (Figure 2C) and $Btk^{-/-}$ cells (data not shown). We also analyzed the effect of the Tec kinase inhibitor LFM-A13 (Mahajan et al., 1999), which was designed to specifically bind the ATP-binding site of Btk,

(D) Microradiograph of the femur of WT, $Tec^{-/-}$, $Btk^{-/-}$, and $Tec^{-/-}Btk^{-/-}$ mice.

(E) Microcomputed tomography of the epiphyseal region of the femurs of WT and $Tec^{-/-}Btk^{-/-}$ mice.

(F) Histological analysis of the proximal tibiae of WT and $Tec^{-/-}Btk^{-/-}$ mice (upper, TRAP/hematoxylin; lower, toluidine blue stainings). Note that the number of TRAP-positive cells is markedly decreased in $Tec^{-/-}Btk^{-/-}$ mice. The bone marrow is filled with unresorbed bone, in which cartilage remnants (arrowheads) characteristic of osteopetrosis are observed.

(G and H) (G) Bone volume and parameters for osteoclastic bone resorption and (H) parameters for osteoblastic bone formation in the bone morphometric analysis of WT and $Tec^{-/-}Btk^{-/-}$ mice. $^{*}p < 0.05$; $^{**}p < 0.01$; $^{***}p < 0.005$; n.s., not significant (throughout the paper).

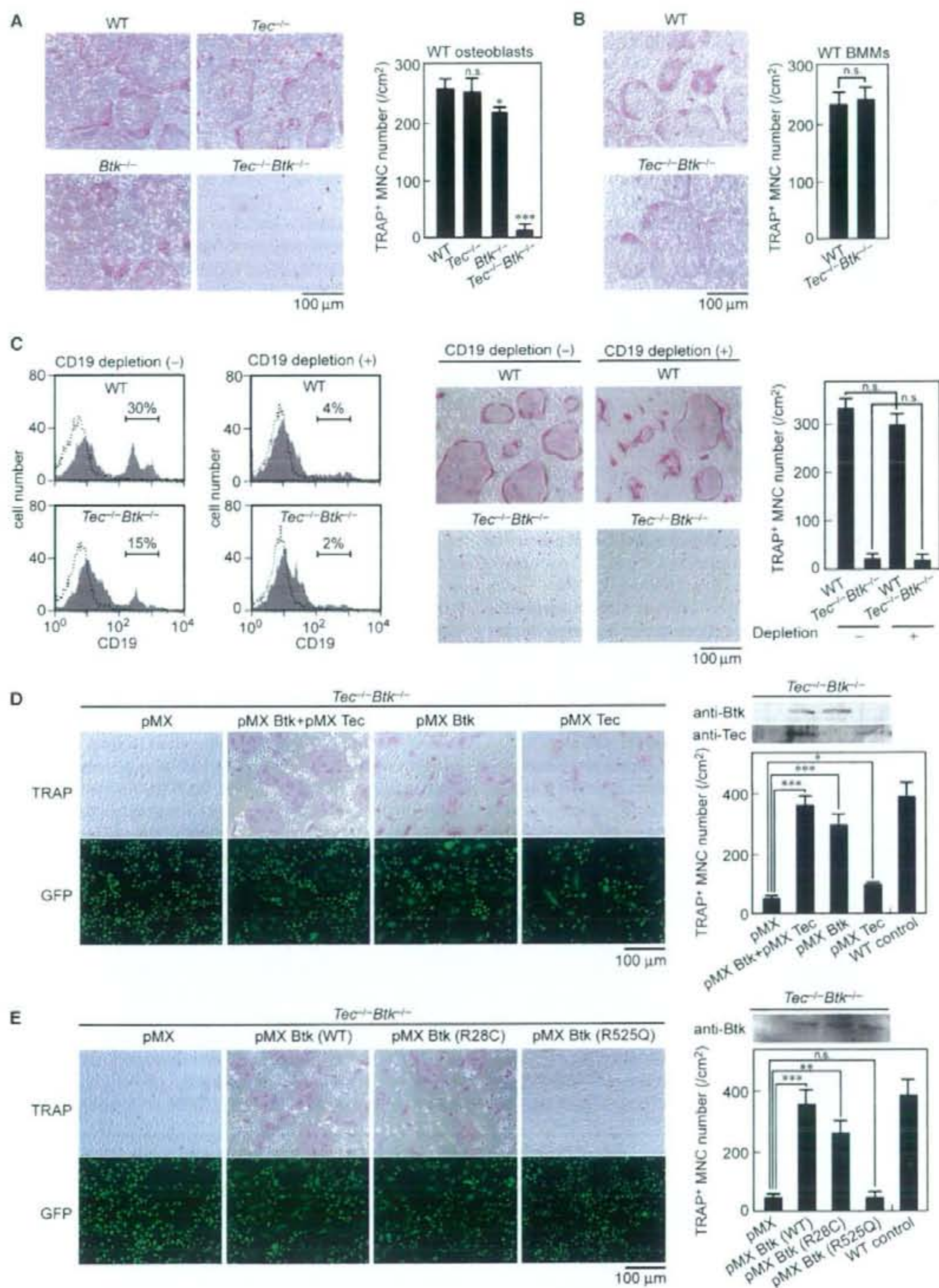
A
WT
Tec-/-
Btk-/-
Tec-/-Btk-/-
100 μm
WT osteoblasts
TRAP+ MNC number (/cm2)
B
WT
Tec-/-Btk-/-
WT BMMs
C
CD19 depletion (-)
CD19 depletion (+)
cell number
CD19
30%
15%
4%
2%
Depletion
D
pMX
pMX Btk+pMX Tec
pMX Btk
pMX Tec
TRAP
GFP
anti-Btk
anti-Tec
WT control
E
pMX Btk (WT)
pMX Btk (R28C)
pMX Btk (R525Q)

and which was revealed subsequently to suppress other Tec kinases additionally (Fernandes et al., 2005), on osteoclast differentiation. LFM-A13 strongly inhibited RANKL-induced osteoclastogenesis (Figure 2D) and NFATc1 induction (data not shown). In contrast, this compound only slightly affected the bone resorption activity of osteoclasts (Figure S2). Importantly, phosphorylation of Btk and Tec was induced by RANKL stimulation in BMMs (Figure 2E). Thus, the tyrosine kinases Btk and Tec are activated by RANKL and play a crucial role in RANKL-induced signal transduction during osteoclastogenesis.

Impaired Osteoclastogenesis in *Tec*$^{-/-}$*Btk*$^{-/-}$ Mice Caused by a Cell-Autonomous Mechanism

To determine whether impaired osteoclastogenesis in *Tec*$^{-/-}$*Btk*$^{-/-}$ mice is caused by a cell-autonomous mechanism, we evaluated the osteoclastogenesis in the coculture system of bone marrow cells with osteoblasts. In the coculture of bone marrow cells derived from mutant mice with WT osteoblasts, osteoclast formation was not severely affected in *Tec*$^{-/-}$ or *Btk*$^{-/-}$ cells but was almost abrogated in *Tec*$^{-/-}$*Btk*$^{-/-}$ cells (Figure 3A). In contrast, *Tec*$^{-/-}$*Btk*$^{-/-}$ osteoblasts were normally able to support osteoclastogenesis of WT bone marrow cells (Figure 3B). These results suggest that the impaired osteoclastogenesis in *Tec*$^{-/-}$*Btk*$^{-/-}$ mice is caused by a defect in osteoclast precursor cells. Consistent with the observation that the *Btk*$^{-/-}$ mice have a normal number of osteoclasts in vivo (Figure S1), *Btk*$^{-/-}$ cells differentiate into osteoclasts in the coculture system essentially in a normal manner (Figure 3A), indicating that the larger contribution of Btk is observed only under limited in vitro conditions, including the RANKL/M-CSF-stimulated BMM culture system (Figure 2A). Since a similar observation has been made in *DAP12*$^{-/-}$ cells (Koga et al., 2004), we infer that Btk is more closely associated with the DAP12-dependent pathway.

Since *Tec*$^{-/-}$*Btk*$^{-/-}$ mice have almost no B cells and exhibit severe immunodeficiency (but their T cells are not affected) (Ellmeier et al., 2000), it is possible that the impaired osteoclastogenesis is influenced by differences in the B cell number in the bone marrow. Therefore, we examined whether depletion or addition of CD19^{+} B cells had any effect on osteoclastogenesis from bone marrow cells containing B cells. Osteoclast differentiation was not influenced by the coexistence of B cells in either WT or *Tec*$^{-/-}$*Btk*$^{-/-}$ cells (Figure 3C). Taken together, these results indicate that the impaired osteoclastogenesis in *Tec*$^{-/-}$*Btk*$^{-/-}$ mice is not related to an abnormality of other cell types such as osteoblasts or B cells, supporting the notion that the impaired osteoclast differentiation is caused by a cell-autonomous mechanism.

Consistent with this notion, retrovirus-mediated expression of Btk and Tec almost completely recovered the osteoclast differentiation in *Tec*$^{-/-}$*Btk*$^{-/-}$ BMMs. The introduction of Btk into *Tec*$^{-/-}$*Btk*$^{-/-}$ BMMs by retroviral transfer markedly rescued the differentiation blockade, but that of Tec rescued it to a lesser extent (Figure 3D). This result is consistent with the dominant role of Btk in osteoclastogenesis in the BMM culture system (Figure 2A). Tec family kinases contain a pleckstrin-homology (PH) domain that binds to phosphatidylinositol-3,4,5-triphosphate (PtdIns[3,4,5]P_3), a lipid product of phosphoinositide 3-kinase, a Tec homology domain, and a carboxyl-terminal kinase domain (Schmidt et al., 2004). A kinase-inactive mutant of Btk (R525Q) that carries a mutation in the kinase domain (Takata and Kurosaki, 1996) did not rescue the osteoclast differentiation blockade, but another mutant (R28C) that harbors a mutation in the PH domain (Takata and Kurosaki, 1996), which causes a certain type of XLA in humans (Tsukada et al., 1993), exhibited a capacity for rescue comparable to the WT Btk (Figure 3E). The results suggest that the function of Btk in osteoclastogenesis requires its kinase activity but does not completely depend on the interaction with PtdIns(3,4,5)P_3 through the PH domain.

Tec Kinases Link the RANK Signal to the Phosphorylation of PLCγ

How does deficiency of Btk and Tec affect the osteoclastogenic signaling pathways? To address these issues by a systems biology approach, we utilized a systematic protein-protein interaction database created by the Genome Network Project (http://genomenetwork.nig.ac.jp/index.html), in which our laboratory has served as a working member. From this database, we extracted the protein-protein interaction network related to the two major signaling pathways regulating osteoclastogenesis, the RANK and ITAM pathways, with which we merged our original data on the increase in mRNA expression after RANKL stimulation (Figure 4A). The RANK-associated gene network included TRAF6, NF-κB, and mitogen-activated protein kinase (MAPK), whereas the ITAM (DAP12/FcRγ)-associated gene network included Syk, PLCγ, and Btk/Tec. As expected, the expression of many RANK-associated molecules was upregulated by RANKL stimulation. Interestingly, the expression of many of the genes in the ITAM-associated gene network was also upregulated by RANKL stimulation.

Based on these results, together with the observation that Btk and Tec were activated by RANKL (Figure 2E), we hypothesized that Btk and Tec are the molecules that bridge the RANK and ITAM pathways to activate calcium signaling. Notably, RANKL-induced tyrosine phosphorylation of PLCγ1 and PLCγ2 was markedly suppressed in *Tec*$^{-/-}$*Btk*$^{-/-}$ cells (Figure 4B). Furthermore, the RANKL-induced calcium oscillation required for *NFATc1* induction was barely observed in *Tec*$^{-/-}$*Btk*$^{-/-}$ cells (Figure 4C). In contrast, we observed a normal level of RANKL-induced activation of MAPKs (ERK, JNK, p38), IκB kinase α (IKKα),

Figure 3. Impaired Osteoclastogenesis in *Tec*$^{-/-}$*Btk*$^{-/-}$ Mice Caused by a Cell-Autonomous Mechanism

(A) Osteoclast differentiation from WT, *Tec*$^{-/-}$, *Btk*$^{-/-}$, and *Tec*$^{-/-}$*Btk*$^{-/-}$ bone marrow cells in the coculture system with WT osteoblasts.

(B) Osteoclast differentiation from WT bone marrow cells in the coculture system with WT or *Tec*$^{-/-}$*Btk*$^{-/-}$ osteoblasts.

(C) Effect of CD19^{+} B cell depletion on osteoclast differentiation. The number of CD19^{+} cells before and after depletion of CD19^{+} B cells in bone marrow cells derived from WT or *Tec*$^{-/-}$*Btk*$^{-/-}$ mice (left). Osteoclast differentiation from WT and *Tec*$^{-/-}$*Btk*$^{-/-}$ BMMs after depletion of CD19^{+} B cells in response to RANKL and M-CSF (right).

(D) Effects of retroviral expression of Tec (pMX Tec) and/or Btk (pMX Btk) on osteoclastogenesis from *Tec*$^{-/-}$*Btk*$^{-/-}$ BMMs stimulated with RANKL and M-CSF.

(E) Effects of retroviral expression of WT Btk or Btk mutants harboring a mutation in the PH domain (R28C) or the kinase domain (R525Q) on osteoclastogenesis from *Tec*$^{-/-}$*Btk*$^{-/-}$ BMMs stimulated with RANKL and M-CSF.

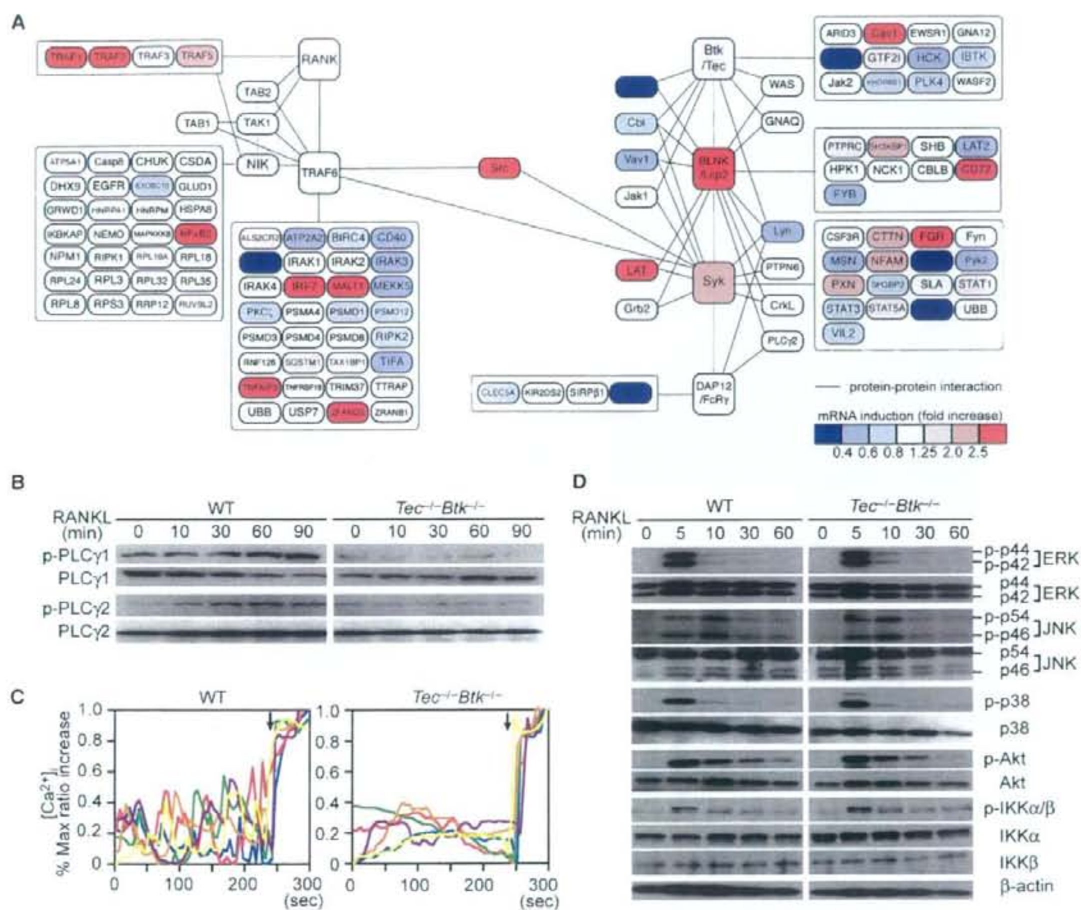

Figure 4. Tec Kinases Mediate Osteoclastogenic Signaling Pathway

(A) Dynamic protein-protein interaction network in osteoclast differentiation. Proteins connected with a black line are interacting partners, and the color indicates how many fold mRNA expression was increased 24 hr after RANKL stimulation.

(B) RANKL-induced PLCγ1 and PLCγ2 phosphorylation in WT and $Tec^{-/-}Btk^{-/-}$ BMMs.

(C) Oscillatory change in the intracellular Ca^{2+} concentration in WT and $Tec^{-/-}Btk^{-/-}$ BMMs after RANKL stimulation. The addition of 10 μM ionomycin at the end of each experiment is indicated by an arrow. Each color indicates a different cell in the same field.

(D) RANKL-induced ERK, JNK, p38, Akt, and IKK phosphorylation in WT and $Tec^{-/-}Btk^{-/-}$ BMMs.

IKKβ, and Akt, all of which are activated downstream of TRAF6 (Wong et al., 1999) (Figure 4D). These results indicate that RANKL-activated Btk and Tec are selectively involved in the phosphorylation of PLCγ, and a defect in calcium signaling causes the impaired *NFATc1* induction in $Tec^{-/-}Btk^{-/-}$ cells. Thus, Btk and Tec link the RANK signal to calcium signaling in the osteoclast lineage.

Tec Kinases Form an Osteoclastogenic Signaling Complex with Scaffold Proteins

Since PLCγ activation is known to be dependent on the ITAM signal, another question arises as to how PLCγ activation is regulated by both RANK and ITAM signals. The ITAM-associated gene network indicates that ITAM associates with Syk, which associates with and phosphorylates scaffold proteins such as BLNK (Ishiai et al., 1999). Because BLNK associates with Btk in a phosphorylation-dependent manner in B cells (Hashimoto et al., 1999), we examined whether RANKL-activated Btk is recruited to BLNK in BMMs. The colocalization of Btk and BLNK was increased, at what appeared to be the plasma membrane, after RANKL stimulation (Figure 5A and Figure S3). This translocation was not observed in $DAP12^{-/-}FcR\gamma^{-/-}$ cells (Figure 5A and Figure S3), suggesting that the ITAM signals are also required for the formation of the Btk-BLNK complex. Consistent with this, immunoblot analysis showed that Btk coimmunoprecipitated with BLNK in BMMs in the presence of RANKL, but

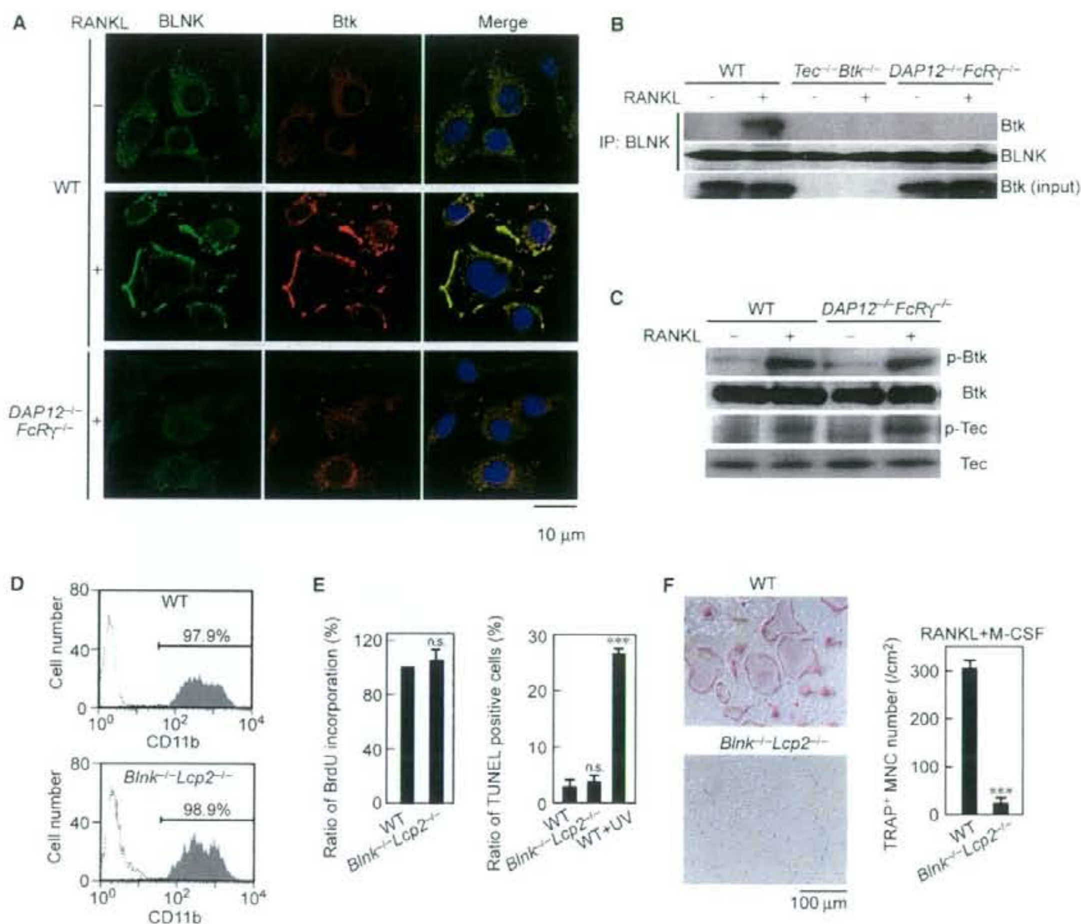

Figure 5. Tec Kinases Form an Osteoclastogenic Signaling Complex with Scaffold Proteins

(A) Immunofluorescence microscopic analysis of colocalization of Btk and BLNK in WT and $DAP12^{-/-}FcR\gamma^{-/-}$ cells 15 min after RANKL stimulation. The nuclei were stained with Hoechst 33342.

(B) Immunoprecipitation analysis of the interaction between Btk and BLNK in WT and $DAP12^{-/-}FcR\gamma^{-/-}$ cells 15 min after RANKL stimulation.

(C) Tyrosine phosphorylation of Tec kinases in WT and $DAP12^{-/-}FcR\gamma^{-/-}$ cells 15 min after RANKL stimulation.

(D) Expression of CD11b in the M-CSF-stimulated bone marrow cells from WT and $Blnk^{-/-}Lcp2^{-/-}$ mice (flow cytometry).

(E) Cell proliferation rate (BrdU incorporation assay) and apoptosis (TUNEL assay) of WT and $Blnk^{-/-}Lcp2^{-/-}$ BMMs stimulated with RANKL and M-CSF.

(F) Osteoclast differentiation from WT and $Blnk^{-/-}Lcp2^{-/-}$ BMMs in response to RANKL and M-CSF.

the association was abrogated in $DAP12^{-/-}FcR\gamma^{-/-}$ cells (Figure 5B). Furthermore, Tec kinases were phosphorylated in response to RANKL, even in $DAP12^{-/-}FcR\gamma^{-/-}$ cells (Figure 5C). Thus, the activation of Btk by RANK and the activation of BLNK by the ITAM signal are both required for the association of Btk with BLNK, which may function as the molecular switch that integrates RANK and ITAM signals.

To further investigate the role of BLNK in osteoclastogenesis, we analyzed osteoclast differentiation in BMMs derived from $Blnk^{-/-}$ mice (Hayashi et al., 2003). However, there was no significant difference in RANKL-induced osteoclastogenesis between the WT and $Blnk^{-/-}$ cells (data not shown), suggesting that another molecule(s) compensates for the loss of BLNK. SLP-76 (encoded by *Lcp2*) is an adaptor protein homologous to BLNK, functioning mainly in T cells (Pivniouk and Geha, 2000). Since there was no significant difference in RANKL-induced osteoclastogenesis between the WT and $Lcp2^{-/-}$ cells (data not shown), we analyzed mice doubly deficient in BLNK and SLP-76 ($Blnk^{-/-}Lcp2^{-/-}$ mice). Although $Blnk^{-/-}$ mice frequently develop acute leukemia (Jumaa et al., 2003), there was a normal number of $CD11b^{+}$ osteoclast precursor cells in the M-CSF-stimulated bone marrow cells from $Blnk^{-/-}Lcp2^{-/-}$ mice (Figure 5D), and

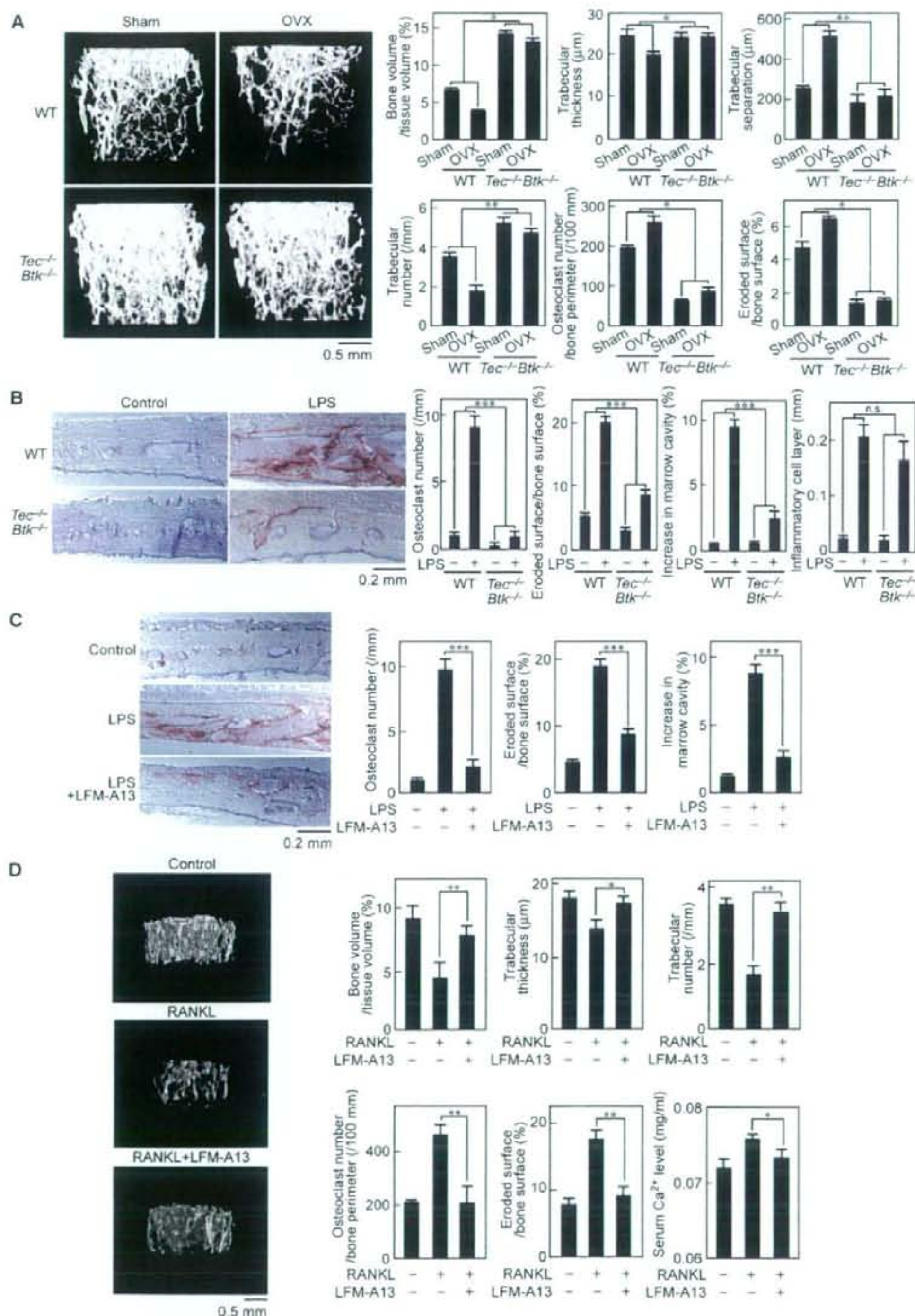
A
Sham
OVX
WT
Tec-/- Btk-/-
0.5 mm
Bone volume /tissue volume (%)
Trabecular thickness (μm)
Trabecular separation (μm)
Trabecular number (/mm)
Osteoclast number /bone perimeter (/100 mm)
Eroded surface /bone surface (%)
Sham OVX Sham OVX
WT Tec-/- Btk-/-
B
Control
LPS
WT
Tec-/- Btk-/-
0.2 mm
Osteoclast number (/mm)
Eroded surface/bone surface (%)
Increase in marrow cavity (%)
Inflammatory cell layer (mm)
n.s.
LPS − + − +
WT Tec-/- Btk-/-
C
Control
LPS
LPS +LFM-A13
0.2 mm
Osteoclast number (/mm)
Eroded surface /bone surface (%)
Increase in marrow cavity (%)
LPS − + +
LFM-A13 − − +
D
Control
RANKL
RANKL+LFM-A13
0.5 mm
Bone volume /tissue volume (%)
Trabecular thickness (μm)
Trabecular number (/mm)
Osteoclast number /bone perimeter (/100 mm)
Eroded surface /bone surface (%)
Serum Ca2+ level (mg/ml)
RANKL − + +
LFM-A13 − − +

the rate of proliferation or apoptosis in *Blnk*$^{-/-}$*Lcp2*$^{-/-}$ BMMs was not significantly different from that in WT BMMs (Figure 5E). We found that in vitro osteoclast differentiation was severely abrogated in *Blnk*$^{-/-}$*Lcp2*$^{-/-}$ BMMs (Figure 5F), suggesting an important role for BLNK and SLP-76 in osteoclast differentiation. Thus, the scaffold proteins, with which the Tec kinases form a complex, have emerged as critical mediators of osteoclastogenic signals. These results further lend support to the crucial role of the RANKL-stimulated formation of the osteoclastogenic complex: the interaction of Tec kinases and their scaffold proteins results in the efficient phosphorylation of PLCγ.

Tec Kinases as Potential Therapeutic Targets for Bone Diseases

To investigate the role of Btk and Tec in the pathological activation of osteoclastogenesis, *Tec*$^{-/-}$*Btk*$^{-/-}$ mice were subjected to an ovariectomy (OVX)-induced model of postmenopausal osteoporosis (Aoki et al., 2006). The bone volume and trabecular bone number/connectivity were significantly reduced by the estrogen withdrawal in WT mice, but such a reduction was observed to a much lesser extent in *Tec*$^{-/-}$*Btk*$^{-/-}$ mice (Figure 6A and Figure S4). An increase in osteoclast number induced by OVX was also much lower in *Tec*$^{-/-}$*Btk*$^{-/-}$ mice (Figure 6A and Figure S4), suggesting a key role of Btk and Tec in the pathological activation of osteoclastogenesis.

Furthermore, *Tec*$^{-/-}$*Btk*$^{-/-}$ mice were subjected to a lipopolysaccharide (LPS)-induced model of inflammatory bone destruction (Takayanagi et al., 2000). *Tec*$^{-/-}$*Btk*$^{-/-}$ mice were protected from the activation of osteoclastogenesis and bone loss (Figure 6B), whereas the formation of an inflammatory cell layer, the number of infiltrated inflammatory cells, IKK activation, and serum levels of TNF-α and IL-6 in *Tec*$^{-/-}$*Btk*$^{-/-}$ mice were not different from those in WT mice (Figure 6B and Figure S5). These results prompted us to examine the therapeutic effects of Tec kinase inhibitor in disease models. Local administration of the Tec kinase inhibitor LFM-A13 had a marked therapeutic effect on the excessive osteoclast formation and bone destruction induced by LPS (Figure 6C) without affecting IKK activation or inflammatory cytokine levels in the serum (Figure S5), although it has been reported that Tec kinases are involved in the activation of immune cells, including lymphocytes and macrophages (Horwood et al., 2003; Mangla et al., 2004). These results suggest that the therapeutic effects of Tec kinase inhibitor in an LPS-induced model are not due to attenuated immune responses but rather are mainly caused by direct inhibitory effects on osteoclast precursor cells. It has been consistently reported that Btk is not essential for LPS-induced inflammatory cytokine production in macrophages under certain conditions (Hata et al., 1998; Perez de Diego et al., 2006).

To determine whether the Tec kinase inhibitor has therapeutic efficacy in a model of osteoporosis, we treated mice that were intraperitoneally injected with GST-RANKL. GST-RANKL injection resulted in an increase in osteoclast number and serum calcium concentration and a decrease in trabecular bone volume, but LFM-A13 treatment significantly ameliorated RANKL-induced bone loss (Figure 6D). These results demonstrate the inactivation of Tec family kinases to be a novel strategy for suppressing osteoclastogenesis in vivo.

DISCUSSION

RANKL-Induced Formation of the Osteoclastogenic Signaling Complex

An osteopetrotic phenotype in *Tec*$^{-/-}$*Btk*$^{-/-}$ mice revealed these two kinases to play a crucial role in the regulation of osteoclast differentiation. Btk and Tec are known to play a key role in proximal BCR signaling (Ellmeier et al., 2000), but this study establishes their crucial role in the integration of the two essential osteoclastogenic signals, RANK and ITAM (Figure 7). Thus, although immune and bone cells share components of signaling cascades, they play distinct roles in each cell type. Furthermore, this study identified an osteoclastogenic signaling complex composed of Tec kinases and adaptor proteins that may provide a new paradigm for the signal transduction mechanism of osteoclast differentiation: ITAM phosphorylation results in the recruitment of Syk, which phosphorylates adaptor proteins such as BLNK and SLP-76, which in turn function as scaffolds to recruit the Tec kinases activated by RANK and PLCγ to the osteoclast signaling complex so as to induce maximal calcium influx.

Such complexes are similar to those formed in the immunological synapse in T cells, which are associated with membrane rafts (Cherukuri et al., 2001). It has been reported that RANK accumulates in membrane rafts, and these specialized domains may play an important role in the RANK signal transduction (Ha et al., 2003). We observed that DAP12, Btk, BLNK, and PLCγ, as well as RANK, were recruited to caveolin-rich membrane domains, which are the crucial signaling domains contained in lipid rafts, after RANKL stimulation (Figure S6). Thus, it is likely that the complex containing both the RANK and ITAM signaling pathways is generated by RANKL stimulation and contributes to the facilitation of the osteoclastogenic signal transduction.

Linkage between Primary Immunodeficiency and Bone Homeostasis

The mutation of *Btk* in humans causes XLA, which is characterized by an arrest in B cell development and immunodeficiency

Figure 6. Tec Kinases as Potential Therapeutic Targets in Bone Diseases

(A) OVX-induced bone loss in WT and *Tec*$^{-/-}$*Btk*$^{-/-}$ mice (evaluated in the femurs and tibiae 3 weeks after sham operation or OVX). The trabecular thickness, separation, and number were obtained from three-dimensional microstructural analysis by microcomputed tomography. Bone volume, osteoclast number, and eroded surface were based on the bone morphometric analysis.

(B) Inflammation-induced bone destruction in WT and *Tec*$^{-/-}$*Btk*$^{-/-}$ mice. Histology of the calvarial bone injected with saline (control) or LPS in WT and *Tec*$^{-/-}$*Btk*$^{-/-}$ mice (TRAP and hematoxylin staining).

(C) Effect of local administration of the Tec kinase inhibitor LFM-A13 (20 mg/kg) on LPS-induced osteoclast formation and bone destruction (TRAP and hematoxylin staining). This inhibitor at this dosage had marginal effects on B cells.

(D) Effect of local administration of LFM-A13 (20 mg/kg) on RANKL-induced osteoclast formation and bone loss. After mice were sacrificed 1.5 hr after the final injection, serum calcium level was measured, and three-dimensional microstructural analysis (femur) and the bone morphometric analysis (tibia) were performed.

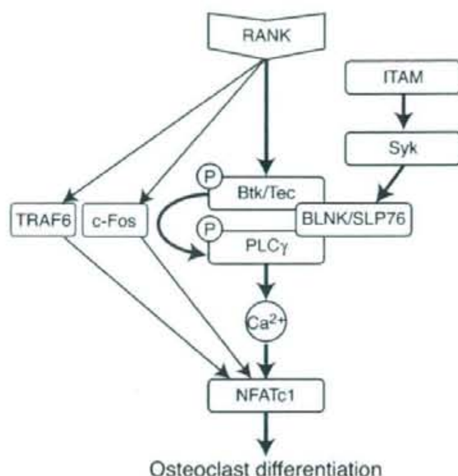

Figure 7. Integration of the RANK and ITAM Signals by Tec Kinases
RANKL binding to RANK results in activation of classical pathways involving TRAF6 and c-Fos. In addition, Tec kinases are phosphorylated by RANK. ITAM phosphorylation results in the recruitment of Syk, leading to activation of adaptor proteins such as BLNK and SLP-76, which function as scaffolds that recruit both Tec kinases and PLCγ to form the osteoclastogenic signaling complex. This complex is crucial for efficient activation of calcium signaling required for the induction and activation of NFATc1, the key transcription factor for osteoclast differentiation.

(Tsukada et al., 1993). Targeted disruption of *Btk* alone did not result in an obvious bone phenotype in mice, and B cell immunoglobulin production was also not severely affected in this strain (Kerner et al., 1995). Therefore, it is possible that the mouse and human utilization of Tec family kinases is not strictly the same. Because immunoglobulin production is completely abrogated in the combined deficiency of Btk and Tec (Ellmeier et al., 2000), $Tec^{-/-}Btk^{-/-}$ mice may serve as a better model of XLA. Currently there is no report on abnormalities of bone metabolism in the XLA patients, but it will be of great significance to analyze bone density and quality in patients with primary immunodeficiencies in the future. These studies, together with others, including recent data on hyper-IgM syndrome (Lopez-Granados et al., 2007), will surely shed light on unexpected aspects of the linkage between the immune and bone systems.

Upstream and Downstream of Tec Kinases in the Osteoclastogenic Signal Transduction

Although phosphorylation of Tec kinases is dependent on Src family kinases in immune cells (Schmidt et al., 2004), c-Src deficiency or inhibition of Src family kinases by PP2 has little effect on osteoclast differentiation (T.K. and H.T., unpublished data). Although it is possible that other Src family members may compensate, to date there has been no clear evidence demonstrating an essential role for Src kinases in osteoclast differentiation; therefore, the kinases that phosphorylate the Tec kinases in osteoclasts remain to be elucidated.

Based on the in vitro data (Figure 4B), the phosphorylation of PLCγ by RANKL is mostly dependent on Btk and Tec. However, osteopetrosis in $Tec^{-/-}Btk^{-/-}$ mice is less severe than that in $DAP12^{-/-}FcR\gamma^{-/-}$ mice, and pathological bone loss is not completely abrogated in the $Tec^{-/-}Btk^{-/-}$ mice or the Tec kinase inhibitor-treated mice. It is conceivable that the loss of Btk and Tec is partly compensated by other Tec kinases or that an alternative kinase(s) partially functions as a PLCγ kinase during osteoclastogenesis.

Despite the crucial role of BLNK and SLP-76 in osteoclast differentiation in vitro, bone mineral density was not markedly increased in $Blnk^{-/-}Lcp2^{-/-}$ mice (M.S., T.K., and H.T., unpublished data). One explanation for this discrepancy is that BLNK and SLP-76 do play a substantially important role, but another adaptor molecule, such as cytokine-dependent hematopoietic cell linker (Clnk), may compensate for the loss in vivo. Although further studies are necessary to elucidate the mechanism(s), it is likely that membrane-bound or soluble factors, which induce or activate Clnk, are compensatorily upregulated only in vivo. In addition, as $Blnk^{-/-}Lcp2^{-/-}$ mice develop acute leukemia at a very high frequency (more than 90%; D.K., unpublished data), the onset of acute leukemia may affect bone homeostasis by producing soluble factors that activate osteoclastogenesis or inhibit osteoblastic bone formation.

Tec Family Kinases as Therapeutic Targets for Bone Diseases

$Tec^{-/-}Btk^{-/-}$ mice are resistant to OVX-induced bone loss, but $DAP12^{-/-}FcR\gamma^{-/-}$ mice, which exhibit more severe osteopetrosis, do lose bone after OVX in certain bones (Wu et al., 2007). These results suggest that osteoclastogenesis under pathological conditions is dependent on a signaling mechanism distinct from that in physiological bone remodeling. Whatever the detailed mechanism, the results indicate that the Tec kinases offer some auspicious therapeutic targets in the treatment of metabolic and inflammatory bone diseases (see Figure 6).

Considering the severe immunodeficiency in XLA, careful attention would obviously have to be given to side effects on other cell types, including B cells, if Tec kinases were systemically inhibited in order to treat metabolic bone diseases. In the case of inflammatory bone diseases such as rheumatoid arthritis, certain immunosuppressants have already been successfully utilized in the clinic, so the inhibition of these kinases may prove to be a potentially effective strategy for preventing bone destruction associated with inflammation. Undoubtedly, the suppression of molecules shared by immune and bone cells will require a very careful evaluation in both systems prior to any clinical application, but these efforts will be rewarded by the provision of a molecular basis for novel drug design in the future.

EXPERIMENTAL PROCEDURES

Mice and Analysis of Bone Phenotype

We previously described the generation of $Tec^{-/-}Btk^{-/-}$ (Ellmeier et al., 2000) and $DAP12^{-/-}FcR\gamma^{-/-}$ (Koga et al., 2004) mice. $Blnk^{-/-}$ (Hayashi et al., 2003) and $Lcp2^{-/-}$ (Pivniouk et al., 1998) mice were described previously. Histomorphometric and microradiographic examinations were performed as described (Koga et al., 2004).

In Vitro Osteoclast Formation, Ca^{2+} Measurement, and GeneChip Analysis

Bone marrow cells were cultured with 10 ng/ml M-CSF (R & D Systems) for 2 days, and they were used as BMMs. BMMs were cultured with 50 ng/ml RANKL (Peprotech) and 10 ng/ml M-CSF for 3 days. RANKL and M-CSF were added at these concentrations unless otherwise indicated. In the coculture system, bone marrow cells were cultured with calvarial osteoblasts with 10^{-8} M 1,25-dihydroxyvitamin D_3 and 10^{-6} M prostaglandin E_2. TRAP-positive MNCs (TRAP⁺ MNCs, more than three nuclei) were counted. Proliferation rate was determined 24 hr after RANKL stimulation using Cell Proliferation ELISA Kit (Roche). Apoptosis was assayed 24 hr after RANKL stimulation using In Situ Cell Death Detection Kit (Roche). In Figure 2D, LFM-A13 (Calbiochem) was added at the same time as RANKL. Concentration of intracellular calcium was measured and GeneChip analysis was performed as described (Takayanagi et al., 2002).

Retroviral Gene Transfer

Retroviral vectors, pMX-Tec-IRES-GFP, pMX-Btk-IRES-GFP, pMX-Btk (R28C)-IRES-GFP, and pMX-Btk (R525Q)-IRES-GFP, were constructed by inserting cDNA fragments of Tec, Btk, Btk (R28C), or Btk (R525Q) (Takata and Kurosaki, 1996) into pMX-IRES-EGFP. Retrovirus packaging was performed by transfecting Plat-E cells with the plasmids as described previously (Morita et al., 2000). After 6 hr inoculation, BMMs were stimulated with RANKL for 3 days.

Depletion of $CD19^+$ B Cells

Bone marrow cells contain $CD19^+$ cells at the ratio of about 30% in WT mice and about 15% in $Tec^{-/-}Btk^{-/-}$ mice. $CD19^+$ cells were depleted with a magnetic sorter and anti-CD19 microbeads (MACS; Miltenyi Biotec). The purity was confirmed by FACS, and the population of $CD19^+$ B cells was less than 5% in these preparations.

Immunoblot Analysis, Immunofluorescence Staining, and Flow Cytometry

After being stimulated with RANKL and M-CSF, BMMs were harvested and cell lysates were subjected to immunoblot or immunoprecipitation analyses with specific antibodies against Tec (Mano et al., 1995), Btk, NFATc1, PLCγ1, BLNK, DAP12, β-actin (Santa Cruz), phospho-PLCγ2, PLCγ2, phospho-ERK, ERK, phospho-p38, p38, phospho-JNK, JNK, phospho-Akt, Akt, phospho-IKKα/β, IKKα, IKKβ (Cell Signaling), phospho-PLCγ1 (Biosource International), Itk, 4G10 (Upstate), and phospho-Btk (BD Biosciences). For immunofluorescence staining, cells were fixed with 4% paraformaldehyde, permeabilized, and then treated with the indicated specific antibodies followed by staining with Alexa Fluor 488- or 546-labeled secondary antibody (Molecular Probes). For flow cytometry, bone marrow cells were incubated with the anti-CD11b antibody (BD Biosciences) or control rat IgG for 30 min followed by staining with PE-conjugated anti-rat IgG antibody.

Ovariectomy-Induced Bone Loss

Seven-week-old female mice were ovariectomized under anesthesia. Three or 8 weeks after surgery, all of the mice were sacrificed and subjected to histomorphometric and microradiographic examinations. Parameters for trabecular bone (thickness, separation, and number) were calculated on the basis of data obtained from microcomputed tomography analysis as described (Aoki et al., 2006).

LPS-Induced Bone Destruction

Seven-week-old female mice were administered with a local calvarial injection of LPS (Sigma) at 25 mg/kg body weight with a simultaneous injection of LFM-A13 (20 mg/kg body weight) or saline and were analyzed after 5 days as described (Takayanagi et al., 2000). For the detection of IKK phosphorylation, the calvarial tissues were homogenized 15 min after LPS injection, and lysates were subjected to immunoblot analysis. The serum levels of TNF-α and IL-6 (30 min after LPS injection) were measured by ELISA kits (R & D Systems).

RANKL-Induced Bone Loss

Seven-week-old C57BL/6 female mice were intraperitoneally injected with 20 μg of GST or GST-RANKL (Oriental Yeast Co., Ltd.) three times at intervals of 24 hr. LFM-A13 (20 mg/kg body weight) or saline was injected 1 hr prior to GST-RANKL treatment. One and a half hours after the final injection, all of the mice were sacrificed and subjected to histomorphometric and microradiographic examinations. The serum level of Ca^{2+} was measured by Calcium C (Wako).

Statistical Analysis

All data are expressed as the mean ± SEM (n = 5). Statistical analysis was performed by using Student's t test or ANOVA followed by Bonferroni test when applicable ($^*p < 0.05$; $^{**}p < 0.01$; $^{***}p < 0.005$; n.s., not significant). Results are representative examples of more than four independent experiments. In Figure 6, statistical analysis was performed between WT and $Tec^{-/-}Btk^{-/-}$ mice (n = 5 per group) on the fold increase of each parameter.

SUPPLEMENTAL DATA

Supplemental Data include six figures and can be found with this article online at http://www.cell.com/cgi/content/full/132/5/794/DC1/.

ACKNOWLEDGMENTS

We thank T. Kitamura, H. Mano, K. Mori, Y. Tomimori, H. Yanagawa, and E. Miyamoto for reagents and technical advice. We also thank M. Isobe-Ohba, T. Nakashima, M. Asagiri, K. Nishikawa, H.J. Gober, K. Kuroda, S. Ochi, Y. Suzuki, and H. Murayama for helpful discussion and assistance. This work was supported in part by a Grant-in-Aid for Creative Scientific Research from the Japan Society for the Promotion of Science (JSPS); grants for the Genome Network Project from the Ministry of Education, Culture, Sports, Science, and Technology of Japan (MEXT); Health Sciences Research grants from the Ministry of Health, Labor, and Welfare of Japan; the Austrian Science Fund and the START Program of the Austrian Ministry of Education, Science, and Culture; and grants from Kanae Foundation for Life and Socio-Medical Science, Tokyo Biochemical Research Foundation, Yokoyama Foundation for Clinical Pharmacology, and Hayashi Memorial Foundation for Female Natural Scientists. No authors have any financial interest related to this work.

Received: June 12, 2007
Revised: November 8, 2007
Accepted: December 27, 2007
Published: March 6, 2008

REFERENCES

Aoki, K., Saito, H., Itzstein, C., Ishiguro, M., Shibata, T., Blanque, R., Mian, A.H., Takahashi, M., Suzuki, Y., Yoshimatsu, M., et al. (2006). A TNF receptor loop peptide mimic blocks RANK ligand-induced signaling, bone resorption, and bone loss. J. Clin. Invest. *116*, 1525–1534.

Asagiri, M., and Takayanagi, H. (2007). The molecular understanding of osteoclast differentiation. Bone *40*, 251–264.

Cherukuri, A., Dykstra, M., and Pierce, S.K. (2001). Floating the raft hypothesis: lipid rafts play a role in immune cell activation. Immunity *14*, 657–660.

Ellmeier, W., Jung, S., Sunshine, M.J., Hatam, F., Xu, Y., Baltimore, D., Mano, H., and Littman, D.R. (2000). Severe B cell deficiency in mice lacking the tec kinase family members Tec and Btk. J. Exp. Med. *192*, 1611–1624.

Faccio, R., Zou, W., Colaianni, G., Teitelbaum, S.L., and Ross, F.P. (2003). High dose M-CSF partially rescues the Dap12−/− osteoclast phenotype. J. Cell. Biochem. *90*, 871–883.

Fernandes, M.J., Lachance, G., Pare, G., Rollet-Labelle, E., and Naccache, P.H. (2005). Signaling through CD16b in human neutrophils involves the Tec family of tyrosine kinases. J. Leukoc. Biol. *78*, 524–532.

Grimbacher, B., Holland, S.M., Gallin, J.I., Greenberg, F., Hill, S.C., Malech, H.L., Miller, J.A., O'Connell, A.C., and Puck, J.M. (1999). Hyper-IgE syndrome with recurrent infections—an autosomal dominant multisystem disorder. N. Engl. J. Med. *340*, 692–702.

Ha, H., Kwak, H.B., Lee, S.K., Na, D.S., Rudd, C.E., Lee, Z.H., and Kim, H.H. (2003). Membrane rafts play a crucial role in receptor activator of nuclear factor κB signaling and osteoclast function. J. Biol. Chem. *278*, 18573–18580.

Hashimoto, S., Iwamatsu, A., Ishiai, M., Okawa, K., Yamadori, T., Matsushita, M., Baba, Y., Kishimoto, T., Kurosaki, T., and Tsukada, S. (1999). Identification of the SH2 domain binding protein of Bruton's tyrosine kinase as BLNK—functional significance of Btk-SH2 domain in B-cell antigen receptor-coupled calcium signaling. Blood *94*, 2357–2364.

Hata, D., Kawakami, Y., Inagaki, N., Lantz, C.S., Kitamura, T., Khan, W.N., Maeda-Yamamoto, M., Miura, T., Han, W., Hartman, S.E., et al. (1998). Involvement of Bruton's tyrosine kinase in FcεRI-dependent mast cell degranulation and cytokine production. J. Exp. Med. *187*, 1235–1247.

Hayashi, K., Yamamoto, M., Nojima, T., Goitsuka, R., and Kitamura, D. (2003). Distinct signaling requirements for Dμ selection, IgH allelic exclusion, pre-B cell transition, and tumor suppression in B cell progenitors. Immunity *18*, 825–836.

Horton, J.E., Raisz, L.G., Simmons, H.A., Oppenheim, J.J., and Mergenhagen, S.E. (1972). Bone resorbing activity in supernatant fluid from cultured human peripheral blood leukocytes. Science *177*, 793–795.

Horwood, N.J., Mahon, T., McDaid, J.P., Campbell, J., Mano, H., Brennan, F.M., Webster, D., and Foxwell, B.M. (2003). Bruton's tyrosine kinase is required for lipopolysaccharide-induced tumor necrosis factor alpha production. J. Exp. Med. *197*, 1603–1611.

Ishiai, M., Kurosaki, M., Pappu, R., Okawa, K., Ronko, I., Fu, C., Shibata, M., Iwamatsu, A., Chan, A.C., and Kurosaki, T. (1999). BLNK required for coupling Syk to PLCγ2 and Rac1-JNK in B cells. Immunity *10*, 117–125.

Jumaa, H., Bossaller, L., Portugal, K., Storch, B., Lotz, M., Flemming, A., Schrappe, M., Postila, V., Riikonen, P., Pelkonen, J., et al. (2003). Deficiency of the adaptor SLP-65 in pre-B-cell acute lymphoblastic leukaemia. Nature *423*, 452–456.

Karsenty, G., and Wagner, E.F. (2002). Reaching a genetic and molecular understanding of skeletal development. Dev. Cell *2*, 389–406.

Kerner, J.D., Appleby, M.W., Mohr, R.N., Chien, S., Rawlings, D.J., Maliszewski, C.R., Witte, O.N., and Perlmutter, R.M. (1995). Impaired expansion of mouse B cell progenitors lacking Btk. Immunity *3*, 301–312.

Kirchner, S.G., Sivit, C.J., and Wright, P.F. (1985). Hyperimmunoglobulinemia E syndrome: association with osteoporosis and recurrent fractures. Radiology *156*, 362.

Koga, T., Inui, M., Inoue, K., Kim, S., Suematsu, A., Kobayashi, E., Iwata, T., Ohnishi, H., Matozaki, T., Kodama, T., et al. (2004). Costimulatory signals mediated by the ITAM motif cooperate with RANKL for bone homeostasis. Nature *428*, 758–763.

Lopez-Granados, E., Temmerman, S.T., Wu, L., Reynolds, J.C., Follmann, D., Liu, S., Nelson, D.L., Rauch, F., and Jain, A. (2007). Osteopenia in X-linked hyper-IgM syndrome reveals a regulatory role for CD40 ligand in osteoclastogenesis. Proc. Natl. Acad. Sci. USA *104*, 5056–5061.

Mahajan, S., Ghosh, S., Sudbeck, E.A., Zheng, Y., Downs, S., Hupke, M., and Uckun, F.M. (1999). Rational design and synthesis of a novel anti-leukemic agent targeting Bruton's tyrosine kinase (BTK), LFM-A13. J. Biol. Chem. *274*, 9587–9599.

Mangla, A., Khare, A., Vineeth, V., Panday, N.N., Mukhopadhyay, A., Ravindran, B., Bal, V., George, A., and Rath, S. (2004). Pleiotropic consequences of Bruton tyrosine kinase deficiency in myeloid lineages lead to poor inflammatory responses. Blood *104*, 1191–1197.

Mano, H., Yamashita, Y., Sato, K., Yazaki, Y., and Hirai, H. (1995). Tec protein-tyrosine kinase is involved in interleukin-3 signaling pathway. Blood *85*, 343–350.

Mao, D., Epple, H., Uthgenannt, B., Novack, D.V., and Faccio, R. (2006). PLCγ2 regulates osteoclastogenesis via its interaction with ITAM proteins and GAB2. J. Clin. Invest. *116*, 2869–2879.

Minegishi, Y., Saito, M., Tsuchiya, S., Tsuge, I., Takada, H., Hara, T., Kawamura, N., Ariga, T., Pasic, S., Stojkovic, O., et al. (2007). Dominant-negative mutations in the DNA-binding domain of STAT3 cause hyper-IgE syndrome. Nature *448*, 1058–1062.

Mocsai, A., Humphrey, M.B., Van Ziffle, J.A., Hu, Y., Burghardt, A., Spusta, S.C., Majumdar, S., Lanier, L.L., Lowell, C.A., and Nakamura, M.C. (2004). The immunomodulatory adapter proteins DAP12 and Fc receptor γ-chain (FcRγ) regulate development of functional osteoclasts through the Syk tyrosine kinase. Proc. Natl. Acad. Sci. USA *101*, 6158–6163.

Morita, S., Kojima, T., and Kitamura, T. (2000). Plat-E: an efficient and stable system for transient packaging of retroviruses. Gene Ther. *7*, 1063–1066.

Perez de Diego, R., Lopez-Granados, E., Pozo, M., Rodriguez, C., Sabina, P., Ferreira, A., Fontan, G., Garcia-Rodriguez, M.C., and Alemany, S. (2006). Bruton's tyrosine kinase is not essential for LPS-induced activation of human monocytes. J. Allergy Clin. Immunol. *117*, 1462–1469.

Pivniouk, V.I., and Geha, R.S. (2000). The role of SLP-76 and LAT in lymphocyte development. Curr. Opin. Immunol. *12*, 173–178.

Pivniouk, V., Tsitsikov, E., Swinton, P., Rathbun, G., Alt, F.W., and Geha, R.S. (1998). Impaired viability and profound block in thymocyte development in mice lacking the adaptor protein SLP-76. Cell *94*, 229–238.

Ross, F.P., and Teitelbaum, S.L. (2005). $\alpha_v\beta_3$ and macrophage colony-stimulating factor: partners in osteoclast biology. Immunol. Rev. *208*, 88–105.

Schaeffer, E.M., Debnath, J., Yap, G., McVicar, D., Liao, X.C., Littman, D.R., Sher, A., Varmus, H.E., Lenardo, M.J., and Schwartzberg, P.L. (1999). Requirement for Tec kinases Rlk and Itk in T cell receptor signaling and immunity. Science *284*, 638–641.

Schmidt, U., Boucheron, N., Unger, B., and Ellmeier, W. (2004). The role of Tec family kinases in myeloid cells. Int. Arch. Allergy Immunol. *134*, 65–78.

Soriano, P., Montgomery, C., Geske, R., and Bradley, A. (1991). Targeted disruption of the *c-src* proto-oncogene leads to osteopetrosis in mice. Cell *64*, 693–702.

Takata, M., and Kurosaki, T. (1996). A role for Bruton's tyrosine kinase in B cell antigen receptor-mediated activation of phospholipase C-γ2. J. Exp. Med. *184*, 31–40.

Takayanagi, H. (2007). Osteoimmunology: shared mechanisms and crosstalk between the immune and bone systems. Nat. Rev. Immunol. *7*, 292–304.

Takayanagi, H., Ogasawara, K., Hida, S., Chiba, T., Murata, S., Sato, K., Takaoka, A., Yokochi, T., Oda, H., Tanaka, K., et al. (2000). T-cell-mediated regulation of osteoclastogenesis by signalling cross-talk between RANKL and IFN-γ. Nature *408*, 600–605.

Takayanagi, H., Kim, S., Koga, T., Nishina, H., Isshiki, M., Yoshida, H., Saiura, A., Isobe, M., Yokochi, T., Inoue, J., et al. (2002). Induction and activation of the transcription factor NFATc1 (NFAT2) integrate RANKL signaling in terminal differentiation of osteoclasts. Dev. Cell *3*, 889–901.

Teitelbaum, S.L., and Ross, F.P. (2003). Genetic regulation of osteoclast development and function. Nat. Rev. Genet. *4*, 638–649.

Theill, L.E., Boyle, W.J., and Penninger, J.M. (2002). RANK-L and RANK: T cells, bone loss, and mammalian evolution. Annu. Rev. Immunol. *20*, 795–823.

Tsukada, S., Saffran, D.C., Rawlings, D.J., Parolini, O., Allen, R.C., Klisak, I., Sparkes, R.S., Kubagawa, H., Mohandas, T., Quan, S., et al. (1993). Deficient expression of a B cell cytoplasmic tyrosine kinase in human X-linked agammaglobulinemia. Cell *72*, 279–290.

Walsh, M.C., Kim, N., Kadono, Y., Rho, J., Lee, S.Y., Lorenzo, J., and Choi, Y. (2006). Osteoimmunology: interplay between the immune system and bone metabolism. Annu. Rev. Immunol. *24*, 33–63.

Wong, B.R., Besser, D., Kim, N., Arron, J.R., Vologodskaia, M., Hanafusa, H., and Choi, Y. (1999). TRANCE, a TNF family member, activates Akt/PKB through a signaling complex involving TRAF6 and c-Src. Mol. Cell *4*, 1041–1049.

Wu, Y., Torchia, J., Yao, W., Lane, N.E., Lanier, L.L., Nakamura, M.C., and Humphrey, M.B. (2007). Bone microenvironment specific roles of ITAM adapter signaling during bone remodeling induced by acute estrogen-deficiency. PLoS ONE *2*, e586. 10.1371/journal.pone.0000586.

Available online at www.sciencedirect.com

ScienceDirect

ELSEVIER

IJBCB

The International Journal of Biochemistry & Cell Biology 40 (2008) 598–603

www.elsevier.com/locate/biocel

Signalling networks in focus

Ku, Artemis, and ataxia-telangiectasia-mutated: Signalling networks in DNA damage

Tomohiro Morio [a,1,2], Hyeyoung Kim [b,*,1]

[a] *Department of Pediatrics and Developmental Biology, Tokyo Medical and Dental University, Graduate School of Medicine, Tokyo 113-8519, Japan*

[b] *Department of Food and Nutrition, Brain Korea 21 Project, College of Human Ecology, Yonsei University, Seoul 120-749, Republic of Korea*

Received 15 September 2007; received in revised form 6 December 2007; accepted 17 December 2007
Available online 24 December 2007

Abstract

Cell death linked to DNA damage has been implicated in various diseases caused by environmental stress and infection. Severe DNA damage, which is beyond the capacity of the DNA repair proteins, triggers apoptosis. Accumulation of DNA damage has been proposed to be a principal mechanism of infection, inflammation, cancer, and aging. The most deleterious form of DNA damage is double-strand breaks (DSBs), where ataxia-telangiectasia-mutated (ATM) is the main transducer of the double-strand DNA break signal. Once the DNA is damaged, the DNA repair protein Ku70/80 translocates into the nucleus, a process which may be mediated by ataxia-telangiectasia-mutated, a member of the phosphoinositide-3-kinase-like family. The function and stability of Artemis may also be regulated by ataxia-telangiectasia-mutated through its phosphorylation upon the occurrence of DNA damage. Interestingly, both Artemis and Ku70/80 are substrates of DNA-dependent protein kinase (DNA-PK), another member of the phosphoinositide-3-kinase-like family. In this review, we show how Ku and Artemis function in the DNA damage response and the ataxia-telangiectasia-mutated signaling pathway and discuss potential applications of agents targeting these DNA damage response molecules in the treatment of inflammation and cancer.

© 2007 Elsevier Ltd. All rights reserved.

Keywords: Ku; Artemis; Ataxia-telangiectasia-mutated; DNA damage

Abbreviations: AT, ataxia-telangiectasia; ATM, ataxia-telangiectasia-mutated; ATR, ataxia-telangiectasia and Rad3-related; DNA-PK, DNA-dependent protein kinase; DNA-PKcs, catalytic subunit of DNA-dependent protein kinase; DSBs, double-strand breaks; ROS, reactive oxygen species; NHEJ, non-homologous end joining; HR, homologous recombination; PI-3-kinase, phosphoinositide-3-kinase; CHK2, checkpoint 2 kinase; CdK, cyclin-dependent kinase; M/R/N complex, Mre11/Rad50/NBS1; ATRIP, ATR-interacting protein; XRCC4, X-ray repair complementing defective repair in Chinese hamster cells 4; Mre11, meiotic recombination 11; NBS1, Nijmegen breakage syndrome 1; MDM2, mouse double minute 2; H2AX, histone H2AX; IgCS, immunoglobulin class switch.

* Corresponding author. Tel.: +82 2 2123 3125; fax: +82 2 364 5781.
E-mail addresses: tmorio.ped@tmd.ac.jp (T. Morio), kim626@yonsei.ac.kr (H. Kim).

[1] Both the authors contributed equally to the work.

[2] Tel.: +81 3 5803 5245; fax: +81 3 5803 5245.

1357-2725/$ – see front matter © 2007 Elsevier Ltd. All rights reserved.
doi:10.1016/j.biocel.2007.12.007

Signaling network facts

- Ataxia-telangiectasia-mutated, Ku70/80, and Artemis are involved in the cellular pathways that work to repair DNA double-strand breaks.
- Ku70/80 and Artemis play a crucial role in non-homologous end joining by interacting with other molecules, such as X-ray repair complementing defective repair in Chinese hamster cells 4 (XRCC4), DNA ligase IV, and Cernunnos. Ataxia-telangiectasia-mutated plays a mediating role in homologous recombinational repair of DNA damage by interacting with meiotic recombination 11/Rad50/Nijmegen breakage syndrome 1.
- Functions of Ku70/80 and Artemis are, at least in part, controlled by phosphorylation by DNA-dependent protein kinase. Ku70/80 and Artemis are also substrates of ataxia-telangiectasia-mutated.
- The ataxia-telangiectasia-mutated signal is critical in cell cycle control and in cellular apoptosis via the p53 pathway.
- Ku proteins translocate into the nucleus upon the occurrence of DNA damage, and their nuclear transports are possibly controlled by phosphorylation.
- Nuclear loss of Ku proteins or ataxia-telangiectasia-mutated may be the underlying mechanism of oxidative stress-induced apoptotic cell death.

1. Introduction

Many types of DNA damage can occur within cells, but the most dangerous are double-strand breaks (DSBs). These results from exogenous agents (such as ionizing radiation, chemotherapeutic drugs, and infectious agents), endogenously generated reactive oxygen species (ROS), and mechanical stress acting on the chromosomes. DSBs can also be produced when DNA replication forks encounter DNA single-strand breaks or other lesions. Accumulation of DNA damage, leading to adult stem cell exhaustion, has been proposed as a principal mechanism of aging (Nijnik et al., 2007).

DNA repair proteins, such as DNA-dependent protein kinase (DNA-PK), Ku, and ataxia-telangiectasia-mutated (ATM), have been linked to cellular DNA repair pathways that work to fix DNA DSBs, while ataxia-telangiectasia and Rad3-related (ATR) is activated by many forms of DNA damage. Ku70/80 and Artemis are involved in non-homologous end joining (NHEJ) by interacting with other molecules, such as X-ray repair complementing defective repair in Chinese hamster cells 4 (XRCC4), DNA ligase IV, and Cernunnos. ATM is involved in homologous recombinational repair of DNA damage by interaction with meiotic recombination 11 (Mre11)/Rad50/Nijmegen breakage syndrome 1 (NBS1) (M/R/N complex), cell cycle arrest by the phosphorylation of various molecules such as checkpoint 2 kinase (CHK2), and cellular apoptosis via the p53 pathway.

ATM and DNA-PK may regulate the function of Ku70/80 and Artemis by phosphorylation and/or nuclear transport of Ku proteins and Artemis. In oxidative stress-induced DNA damage, ATM is essential for Ku activation and cell survival. The nuclear loss of Ku 70/80 or ATM is observed upon genotoxic stimuli. Degradation of these molecules may be another underlying mechanism of apoptosis. Further studies on the regulatory mechanisms and signaling networks of DNA damage response molecules are needed to better understand the complex cellular response. This review focuses on the interplay among ATM, Artemis, and Ku70/80 in response to DNA DSBs.

2. Key molecules and functions

2.1. Ku70/80 and DNA damage

The Ku70 (70 kDa) and Ku80 (80 kDa) proteins are DNA-binding regulatory subunits of DNA-PK, which is composed of a 470 kDa catalytic subunit (DNA-PKcs) and Ku proteins. Ku70 and Ku80 initiate the repair process of DNA DSBs, which produce DNA fragmentation, by activating DNA-PK after binding to the DNA DSBs. In addition to the regulatory function of the Ku proteins in DNA-PK, heterodimers of Ku70 and Ku80 have independent DNA repair functions. These include single-stranded DNA-dependent ATPase activity and the binding and repair of broken single-stranded DNA, single-stranded nicks, gaps in DNA, and single-strand-to-double-strand transitions in DNA. The importance of Ku70/80 in DSBs is highlighted by the fact that Ku70-deficient cells have increased ionizing radiosensitivity, defective DNA end-binding activity, and impaired V(D)J recombination. Ku80-null mice display an increase in chromosomal aberrations and malignant transformation

(Difilippantonio et al., 2000; Gu, Jin, Gao, Weaver, & Alt, 1997).

Ku70/80 plays a critical role in the repair of damaged DNA through NHEJ by interacting with XRCC4, Cernunnos, and DNA ligase IV. Phosphorylation of Ku70/80 by DNA-PK controls their localization, DNA binding, and function. DNA-PK phosphorylates Artemis, p53, and histone H2AX, which determine the fate of the cells.

Oxidative stress can be caused by ionizing radiation, cytotoxic drugs, infection, inflammation, cancer, and aging. It leads to the generation of single-strand breaks and DSBs. Oxidative stress-induced DNA damage of haematopoietic stem cells during aging is repaired mainly by NHEJ, in which Ku70/80 has a critical role, but ATM may also be involved (Nijnik et al., 2007). Oxidative injury caused by mild ischemia/reperfusion in the spinal cord induces reversible neurological deficits with increased Ku-DNA binding activity, whereas severe ischemia/reperfusion causes permanent deficits that are accompanied by a decrease in the Ku-DNA binding activity. Therefore, Ku may have a protective role against oxidative injury (Shackelford, Tobaru, Zhang, & Zivin, 1999). Embryonic fibroblasts derived from Ku80-null mice are more susceptible to DNA damage than those from wild-type mice (Arrington et al., 2000), suggesting that a decrease in Ku may be involved in the mechanism of apoptotic cell death. DNA-PKcs is the substrate for caspase-3, which is activated by ischemia/reperfusion and ROS. The reduction in Ku might be induced in a caspase-activating apoptotic pathway after ischemia/reperfusion (Shackelford et al., 1999). Nuclear localization of Ku70 and Ku80 are mediated by two compartments of the nuclear pore-targeting complex, importin α and importin β. Oxidative stress-induced apoptosis is mediated by the activated caspase-3, which degrades Ku70/80 (Song, Lim, Kim, Morio, & Kim, 2003). A decrease in Ku binding to nuclear transporters importin α and importin β results in reduced levels of nuclear Ku70/80 in pancreatic acinar cells. Further studies are required to determine the mechanism of selective reduction of each Ku component upon the occurrence of DNA damage in the cells.

2.2. Ku70/80 as a signaling molecule

Ku70/80 are located in the cytoplasm and on the cell surface (Morio et al., 1999). Ku70 serves as a receptor for *Rickettsia conorii* internalization (Martinez, Seveau, Veiga, Matsuyama, & Cossart, 2005). Ku70/80 is associated with CD40 in the cytoplasm, and CD40 engagement leads to the translocation of Ku70/80 to the cell surface of multiple myeloma cells. In normal human B cells, Ku70/80 resides in the cytoplasm and translocates to the nucleus upon the receipt of the immunoglobulin class switch (IgCS)-inducing signal or upon DNA damage. Since B cells need NHEJ mediated by Ku70/80 when they undergo IgCS (Morio et al., 1999), Ku70/80 may act as a signaling molecule in this cellular process.

Modification of Ku70 and Ku80 takes place when DNA is damaged, and the functional consequences of this modification are of particular interest. Polyglutamine (polyQ) diseases, such as Huntington's disease and Machado-Joseph disease, are caused by the gain of a toxic function by abnormally expanded polyQ tracts. An expanded polyQ of ataxin-3, a gene that causes Machado-Joseph disease, stimulates Ku70 acetylation. This post-translational modification of Ku70 dissociates the proapoptotic protein Bax from Ku70, thereby promoting Bax activation and subsequent cell death. This suggests that cell death is, at least in part, controlled by acetylation of Ku70 (Li et al., 2007). The physiological relevance of Ku phosphorylation is still an enigma. There are four DNA-PK phosphorylation sites on the Ku70/80 heterodimer: serine 6 of Ku70, serine 577 and 580 and threonine 715 of Ku80. However, neither DNA-PK nor ATM is required for phosphorylation of these sites on the Ku70/80 heterodimer *in vivo*. DNA-PK-dependent phosphorylation of Ku70/80 is not required for NHEJ either. The involvement of ATM in Ku70/80 modification awaits further study.

2.3. ATM and Ku70/80

ATM is the protein product of the gene mutated in the multisystem disorder ataxia-telangiectasia (AT), which is characterized by neuronal degeneration, immunodeficiency, chromosomal instability, and a predisposition to cancer formation. ATM is a large molecule with serine/threonine kinase activity, and it functions in DNA damage responses and cell cycle control. DSB recognition is the first step in the DSB damage response and involves activation of ATM and phosphorylation of targets, such as p53, to trigger cell cycle arrest, DNA repair, or apoptosis. The activation of ATR kinase by DSBs also occurs in an ATM-dependent manner. On the other hand, Ku70/80 is known to participate at a later time in the DSB response, recruiting DNA-PKcs to facilitate NHEJ. Recent finding shows that Ku70/80 plays a novel role in modulating ATM-dependent ATR activation during the DSB damage response and confers a protective effect against ATM-independent ATR activation at later stages of the DSB damage response (Tomimatsu et al., 2007). Following exposure to genotoxic stress, proliferating cells actively slow down DNA